INDIAN JOURNAL OF SCIENCE AND TECHNOLOGY

ORIGINAL ARTICLE

OPEN ACCESS

Received: 19/12/2024

Accepted: 24/02/2025

Published: 23/04/2025

Citation: Ramya N, Deivanayaki M (2025) Impact of Soret and Dufour Effects on Casson Nanofluid Flow in a Magnetic Field along with Heat and Mass Transfer. Indian Journal of Science and Technology 18(13): 1059-1070. https://doi.org/10.17485/IJST/v18i13.4028

* **Corresponding author**.

deinayaki@gmail.com

Funding: None

Competing Interests: None

Published By Indian Society for Education and Environment (iSee)

ISSN

Print: 0974-6846

Electronic: 0974-5645

Impact of Soret and Dufour Effects on Casson Nanofluid Flow in a Magnetic Field along with Heat and Mass Transfer

N. Ramya[1], M. Deivanayaki[2]*

1 Research Scholar, Karpagam Academy of Higher Education, Coimbatore, Tami, Nadu, India

2 Associate Professor, Department of Science and Humanities, Karpagam Academy of Higher Education, Coimbatore, Tamil Nadu, India

Abstract

Objective: To investigate the impact of Soret and Dufour on the behaviour of Casson nanofluids over nonlinear stretching surfaces. Also, to study heat transfer efficiency in practical thermal systems and analysing the heat and mass transfer properties. **Method**: The governing equations for fluid flow, heat transfer, and mass transfer are transformed into dimensionless form using similarity transformations. These equations are then solved numerically using MATLAB's bvp4c procedure. **Findings**: Increasing the Soret number enhances fluid concentration, while the Dufour number reduces concentration. The results are validated against existing studies, confirming the reliability of the model. **Novelty**: Casson rheology, micropolar fluid dynamics, and cross-diffusion effects under nonlinear stretching conditions provide a comprehensive framework for understanding non-Newtonian fluid behaviour. The findings offer significant insights for optimizing thermal systems, particularly in heat exchangers and mixing technologies.

Keywords: Soret; Skin friction; Casson nanofluid; Diffusion; Thermal

1 Introduction

Heat exchangers are essential parts of many industries, such as refrigeration, electricity generating, and chemical production. Transferring heat between two or more fluids while maintaining their separation is their main purpose. Heat exchanger efficiency is essential for optimising energy use and enhancing thermal system performance. Improved heat recovery systems, in particular, can greatly benefit power plants and increase overall energy efficiency. Significant knowledge gaps still exist about the combined effects of these fluids, particularly under convection-diffusion situations over stretching surfaces, despite the fact that several research have examined their movement in various contexts. The results advance our knowledge of how these intricate fluids behave in real-world settings. Shaheen et al[(1)] examined how the Soret and Dufour phenomena impact the three-dimensional flow of Casson nanofluids with dust particles and other properties in a permeable medium. The heat and mass transport of Casson micropolar fluid in a magnetic field across a stretching surface Amjad et al, Devi et al and Chun et al[2],[3],[4]. Numerical results on heat transmission in rotating disc flows and Carreau nanofluids examined by Magesh et al and Shevchuk et al[5],[6]. The repercussion of calefaction cause framework over a wedge over permeable space for electrically overriding fluid flow for a magneto hydrodynamic Casson nano fluid with invigoration hall and Soret discussed by Bafakeeh et al[7]. The concussion of non-Newtonian fluid with actinic attitude stays in velocity and thermal effects also investigated by Chandrasekhar et al[8]. The prospect of environmental parameters related to the pace, warmth and absorption are detailed in several visual representations. Algebraic study for the magneto hydro staunches of Casson nanofluid over an inclusive sheet through a permeable medium under chattels of lukewarm emission, Heat-Propagation/dispersion, Joule cooling effect and error boundary circumstances discussed by Kesavaiah et al, Deepthi et al and Ganjikunta et al[9],[10],[11]. The properties of Casson-type nanofluids that extend to flow through porous media on nonlinear resilient surfaces in premises of heat and mass transfer progression analysed by Gopal et al and Rasool et al[12],[13]. Williamson Nano Casson fluid the potential MHD flow and lukewarm deportation is analysed by Jawad et al[14]. The MHD mixed convection flow of Maxwell nanofluid through a permeable material filled with an inverted helix, varying in the boiling point and influenced by Soret phenomena, is analyzed analytically by Kodi et al[15]. The erratic MHD progress of Eyring Powell nano fluid over a slanted permeable sheet along sticky decay, warming by Joules, and uneven metabolic processes at both destinations has been numerically studied by Kumar et al[16]. For the inquiry of the deportation of mass and warmth, ramifications such as variable Hall current, activation energy, and dissemination thermodynamics are also featured by Reddy et al[17]. The substance's mobility was decreased by the Casson factor and slant discussed by Rafque et al, Sutkar et al and Ramya et al[18],[19],[20]. Heat radiation and mass diffusion affect the flow of Casson nanofluid across a slanted stretched surface, with implications for engineering applications involving heat and mass transfer examined Ramya et al[21]. Chemical reaction effects on micropolar fluid and Casson-Williamson nanofluid investigated by Yousef et al[22]. Manohar et al[23] analysed Casson liquid flow in a porous microchannel with hybrid nanoparticles, highlighting enhanced heat transfer due to nanoparticle dispersion and porous medium effects. Ramesh et al[24] examined the squeezing flow of Casson-micropolar nanofluid, showing how slip, suction/injection, and microstructure influence heat and mass transfer dynamics. The study of MHD Casson fluid flow is essential for managing the behaviour of molten metals during manufacturing processes in metallurgical processing, for example. Because of phase-change dynamics and solid particle suspensions, molten metals frequently behave non-Newtonian, much like Casson fluids. By boosting impurity elimination, increasing thermal conductivity, and decreasing turbulence, the application of a magnetic field (MHD effect) affects the metal flow.

Despite the extensive research in individual areas, there is a lack of comprehensive studies that address the combined effects of MHD, Casson nanofluid characteristics, micropolar behaviour, nanofluid dynamics, and convection-diffusion conditions on heat transfer over nonlinear stretching surfaces. This study fills this gap by providing a unified framework to analyse these interactions, offering deeper insights into heat distribution and energy transfer in thermal systems. The novelty of this work lies in its integration of several previously studied, MHD effects, Casson nanofluid dynamics and nanofluid convection-diffusion conditions into a cohesive model. The proposed method's effectiveness is validated through numerical simulations, revealing significant improvements in heat transfer efficiency, as demonstrated by the increase in the Nusselt and Sherwood numbers, as well as a reduction in friction drag. This research is particularly relevant for optimizing thermal systems such as heat exchangers, where multiple factors interact Figure 1.

2 Methodology

Two-dimensional atmospheric MHD flow of Casson nanofluid with tiny particles while the approach of thermostatic in the zone $y > 0$ past an elongated plate, whose power-low rate is interpreted as $u_x = ax$, at which a symbolizes an unbalanced real variety. Figure 1 shows physical representation of the fluid flow. The y-axis is identical to the expanding form, which is arranged to be organized in concert with the x-axis.

The continuum conservation, momentum, energy, microorganism equations[20],[22],[23],

Continuity Equation (Mass Conservation)

$$\frac{\partial u}{\partial x} + \frac{\partial u}{\partial y} = 0$$

where u is the velocity component along the plate, and v is the velocity component normal to the plate.

Momentum Equation (Navier-Stokes Equation)

$$\mathrm{u}\,\frac{\partial u}{\partial x} + \mathrm{v}\,\frac{\partial u}{\partial y} = \nu\left[1+\frac{1}{\beta}\right]\left(\frac{\partial^2 u}{\partial y^2}\right) - \left(\frac{k_1}{\rho}\right)\frac{\partial N}{\partial y} + \left[g\beta_T\left[\mathrm{T}\text{-}\mathrm{T}_\infty\right] + \mathrm{g}\beta_C\left[\mathrm{C}\text{-}\mathrm{C}_\infty\right]\right] - \frac{\sigma B_0^2\,\mathrm{u}}{\rho} \tag{1}$$

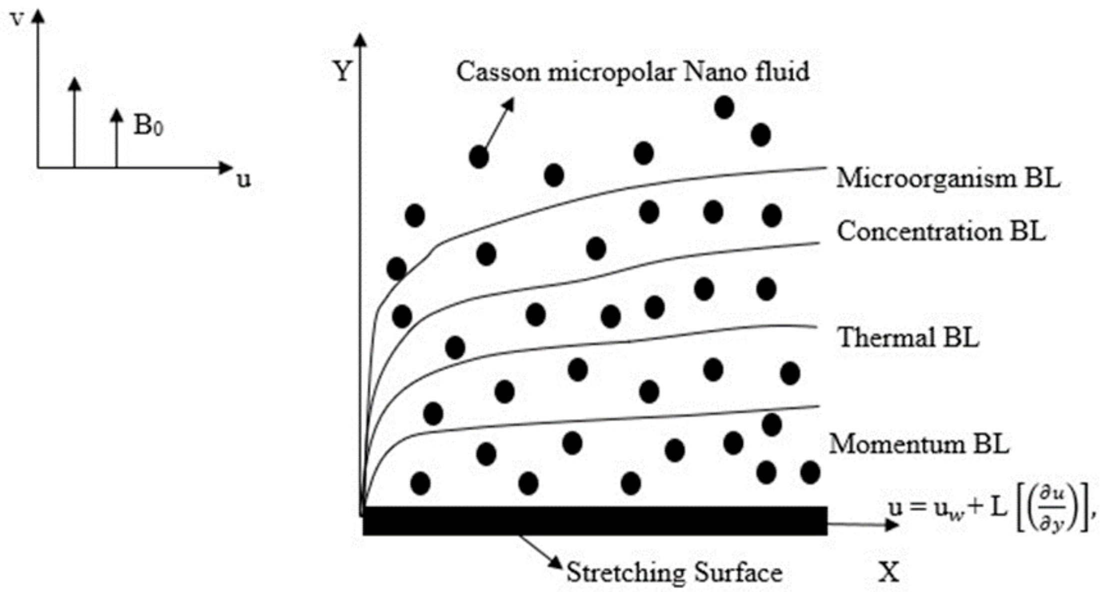

Fig 1. Physical Representation

where ρ is the density, μ is the dynamic viscosity.

Microorganism Equation (Bioconvection Source Term)

$$u\,\frac{\partial N}{\partial x} + v\,\frac{\partial N}{\partial y} = \frac{\gamma}{\rho}\,\frac{\partial^2 N}{\partial y^2} - \left[\frac{k_1}{\rho}\right]\left(2N + \frac{\partial u}{\partial y}\right) \tag{2}$$

where N is microorganism decay coefficient. (2)

Energy Equation (Heat Transfer)

$$\rho C_p\left[u\,\frac{\partial T}{\partial x} + v\,\frac{\partial T}{\partial y}\right] = k\frac{\partial^2 T}{\partial y^2} - \frac{\partial q_r}{\partial y} + q''' + \frac{\rho D_m k_T}{C_s}\,\frac{\partial^2 C}{\partial y^2} \tag{3}$$

where q''' is the heat generation term.

Concentration Equation (Mass Transfer for Nanoparticles and Microorganisms)

$$u\,\frac{\partial C}{\partial x} + v\,\frac{\partial C}{\partial y} = D_m\,\frac{\partial^2 C}{\partial y^2} - k\left[C - C_\infty\right] + \frac{D_m\,k_T}{T_m}\,\frac{\partial^2 T}{\partial y^2} \tag{4}$$

where T_m mean temperature.

Here $u, v, T, g, C, q''', C_s, \beta, T_{\infty}, K_T, C_p, D_m, \rho, \beta_T, v, T_m, C_\infty, \sigma$ are velocity, calefaction, gravitational stimulation, concentration, random thermal criterion, absorption sensitivity, Casson criterion, oblique heat, thermal diffusivity, heat capacity, mass diffusivity, density, coefficient of lukewarm inflation, Radiant heat, thermal conductivity, concentration expansion coefficient, viscosity, average fluid condition, diffusive consolidation, electrical dynamism or chemical reaction parameters.

$$q''' = \frac{k u_w}{x \upsilon}\left(A\left[T_w - T_\infty\right] f' + B\left[T - T_\infty\right]\right)$$

Where $T_w = T_\infty bx$, T_w and T_∞ are Temperature adjacent and a far from the block. Thermal radiation yields following equation:

$$q_r = \frac{-16}{3}\frac{\sigma}{k}\quad T^3\frac{\partial T}{\partial y}$$

The boundary circumstances are[20], [22], [23]

$$\mathrm{u} = \mathrm{u}_w + \mathrm{L}\left[\left(\frac{\partial u}{\partial y}\right)\right], \text{-k}\left[\frac{\partial T}{\partial y}\right] = \mathrm{h}_1\left[T_\infty\text{-T}\right], \text{-N=-m}\left[\frac{\partial u}{\partial y}\right], D_m\left[\frac{\partial C}{\partial y}\right] = \mathrm{h}_2\left[C_w\text{-C}\right] \text{ as y} = 0$$

$$u \to 0, T \to T_\infty, \mathrm{C} \to C_\infty \text{ as y} \to \infty$$

The stream affair $\psi = \psi(x, y)$ for that given as $u = \frac{\partial \psi}{\partial y}, v = \frac{-\partial \psi}{\partial x}$. **Equations (1)-(4)** are reformulated into ordinary equations by employing similar and dimensionless parables as exposed here

$$\eta = \sqrt{\frac{a}{v}}y. \tag{5}$$

The velocity entrails are

$$\begin{aligned} \varphi &= \sqrt{av}xf(\eta), u = \frac{\partial \varphi}{\partial y} = axf'(\eta), N = ax\left(\sqrt{\frac{a}{v}}\right)h(\eta), v = \frac{-\partial \varphi}{\partial x} = \sqrt{av}f(\eta), \\ \theta(\eta) &= \frac{T - T_\infty}{T_w - T_\infty}, \emptyset(\eta) = \frac{C - C_\infty}{C_w - C_\infty}, T = T_\infty\left(1 + (\theta_w - 1)\theta\right) \end{aligned} \tag{6}$$

Using **Equations (5), (6)** convert the governing **Equations (1) to (4)** are transformed as

$$\left[1 + \frac{1}{\beta}\right]f''' + ff' - (f')^2 + Kh' + (Gr_T\theta + Gr_c\phi) - Mf' = 0 \tag{7}$$

$$\left[1 + \frac{K}{2}\right]h'' + fh' - f'h - K\left(2h + f''\right) = 0 \tag{8}$$

$$\begin{aligned} &\left[1 + N_r\{1 + 3(\theta_w - 1) + 3(\theta_w - 1)^2\theta^2 + (\theta_w - 1)^3\theta^3\}\right]\theta'' \\ +\ &N_r\left[(\theta_w - 1)(\theta')^2 + 6(\theta_w - 1)^2\theta(\theta')^2 + 3(\theta_w - 1)^3\theta^2(\theta')^2\right] \\ +\ &P_r f\theta' - P_r f'\theta + A^* f' + B^*\theta + P_r Du\phi'' = 0 \end{aligned} \tag{9}$$

$$\varphi'' + Scf\varphi' - k_r Sc\varphi + ScSr\theta'' = 0 \tag{10}$$

The values are

$$\begin{aligned} Gr_T &= \frac{g\beta_T\left(T_w - T_\infty\right)}{a^2 x}, N_r = \frac{16\sigma T_\infty^3}{3kk}, Gr_C = \frac{g\beta_C\left(C_w - C_\infty\right)}{a^2 x}, \mathrm{Pr} = \frac{\upsilon\rho C_p}{k} = \frac{\mu C_p}{k}, M = \frac{\sigma B_0^2}{a\rho} \\ Sr &= \frac{D_m K_T}{\upsilon T_m}\left(\frac{T_w - T_\infty}{C_w - C_\infty}\right), Sc = \frac{\upsilon}{D_m}, Du = D_m K_T \frac{(C¿¿w - C_\infty)}{C_s C_p \upsilon\left(T_w - T_\infty\right)}¿, K_r = \frac{k}{a} \end{aligned}$$

The diversified boundary settings are as follows,

$$f' = 1 + \gamma f'', f = 0, \theta' = Bi_T(1 - \theta), \phi' = Bi_c(1 - \phi) \text{ as } \eta = 0,$$

$$f'(\eta) = 0, \theta(\eta) = 0, \phi(\eta) = 0 \text{ as } \eta \to \infty$$

It is discovered that the nanofluid model lacks micropolar effects when vertex viscosity or $K = 0$ is eliminated. Friction Drag, the Nusselt incident and the Sherwood incident are described by

$C_{f_x}Re_x^{\frac{1}{2}} = \left(1 + \frac{1}{\beta}\right)f''(0), Nu\Re_x^{\frac{1}{2}} = -\left(1 + N_r(\theta_w)^3\right)\theta'(0), ShRe_x^{-\frac{1}{2}} = -\phi'(0)$. Here, $Re_x = \frac{xu_w}{\upsilon}$ signifies Reynolds Number.

This dimensionless number (Nusselt Number) indicates the enhancement of heat transfer due to convection relative to conduction. Higher values suggest improved thermal performance. The Sherwood Number Similar to the Nusselt number, but for mass transfer, this number reflects the enhancement of mass transfer due to convection compared to diffusion.

3 Solution Methodology

The system of nonlinear ordinary differential equations reduced first order equations for find the numerical solution to our problem. First convert first order equations as,

$$Y_1 = f, Y_2 = f', Y_3 = f'',$$

$$Y_4 = f''' = \left[\frac{1}{\left[1+\frac{1}{\beta}\right]}\right]\left[(Y_2)^2 - Y_1Y_2 - KY9 - (Gr_T\theta + Gr_c\phi) + MY_2\right]$$

$$Y_5 = \theta, Y_6 = \theta',$$

$$\begin{aligned} Y_7 &= \theta'' = \left(\frac{1}{[1+N_r\{1+3(\theta-w-1)+3(\theta_w-1)^2\theta^2+(\theta_w-1)^3\theta^3\}]}\right)(P_rY_2Y_5 \\ &\quad -N_r[(\theta_w-1)(Y_6)^2+6(\theta_w-1)^2\theta(Y_6)^2+3(\theta_w-1)^3\theta^2(Y_6)^2] \\ &\quad -P_rY_1Y_6 - A^*Y_2 - B^*Y_5 - P_rDuY_{10}), \end{aligned}$$

$$Y_8 = \varphi, Y_9 = \varphi',$$

$$Y_{10} = \varphi'' = k_rScY_8 - ScY_1Y_9 - ScSrY_7,$$

$$Y_{12} = h', Y_{13} = h'' = \frac{1}{[1+\frac{K}{2}]}(Y_2Y_{11} - Y_1Y_{12} + K(2Y_{11} + Y_3)$$

Then the boundary conditions become,

$$\begin{aligned} Y_2 &= 1+\gamma Y_3, Y_1 = 0, Y_6 = Bi_T(1-Y_5), Y_7 = Bi_C(1-Y_6) \text{ as } \eta = 0 \\ Y_2 &\to 0, Y_5 \to 0, Y_8 \to 0, Y_9 \to 0 \text{ as } \eta \to \infty \end{aligned}$$

The first order equations solve numerically using MATLAB bvp4c methods to find numerical and graphical solution.

4 Results and Discussion

4.1 Comparison of Results

This section provides a detailed analysis of the results in the context of magnetic parameter (M) influences on $-f''(0)$, focusing on values of M = 0, 1, 3, and 5. The comparative study excludes the effects of Brownian motion and thermophoresis to isolate the magnetic parameter's specific impact. Table **1** shows that the findings align with those of earlier works[22], demonstrating minimal residual errors and confirming the accuracy of the current numerical method, which employs MATLAB's bvp4c solver for boundary value problems. The precision of numerical solutions, consistency with previously validated results[22], and the sensitivity of the model to variations in the magnetic parameter. This study's results emphasize its contribution to advancing heat transfer and mixing technologies Table 1.

The nonlinear equations are naked numerically by bvp4c method. About the graphical results considered $\beta = 1.3, Gr_T = 0.7, M = 1.5, Nr = 0.1, A*B*0.1, \Pr = 7, \theta_w = 2, Gr_c = 0.7, BiT = 2, BiC = 2, Sc = 0.5, Kr = 0.1, Sr = 0.1$ and Du = 0.1. In the visual representation , $f'(\eta), \theta(\eta), \phi(\eta)$ and $h(\eta)$ represent the flow fields curves respectively. Graph Results discussed on θ_w linear and nonlinear values. Figures 2 and 4 ritual that the possessions of β on the $f'(\eta)$ and $h(\eta)$. $f'(\eta)$ and $h(\eta)$

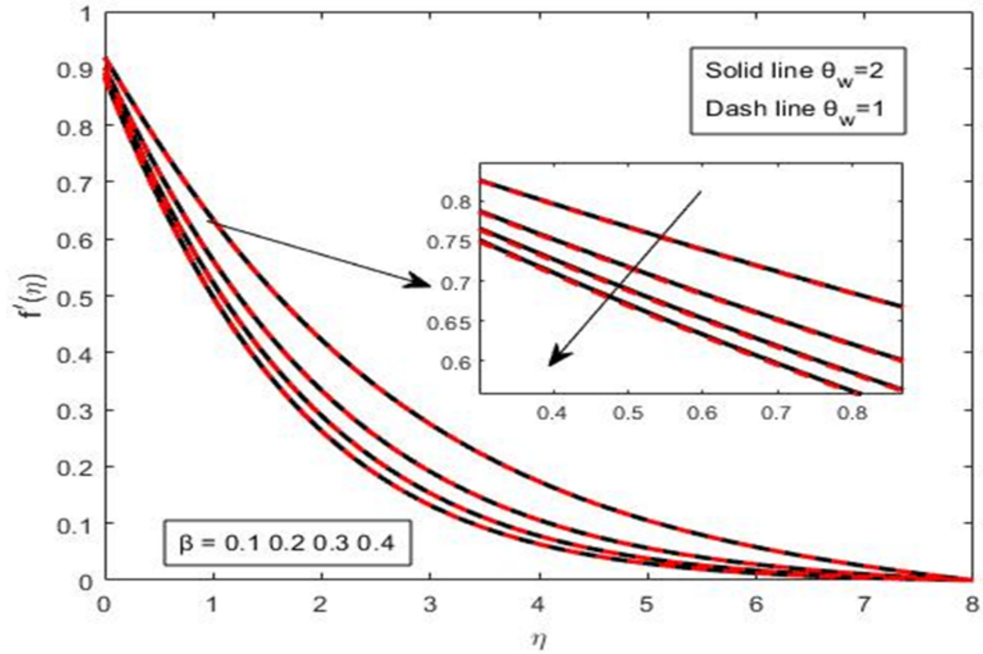

Fig 2. Results of β on Velocity

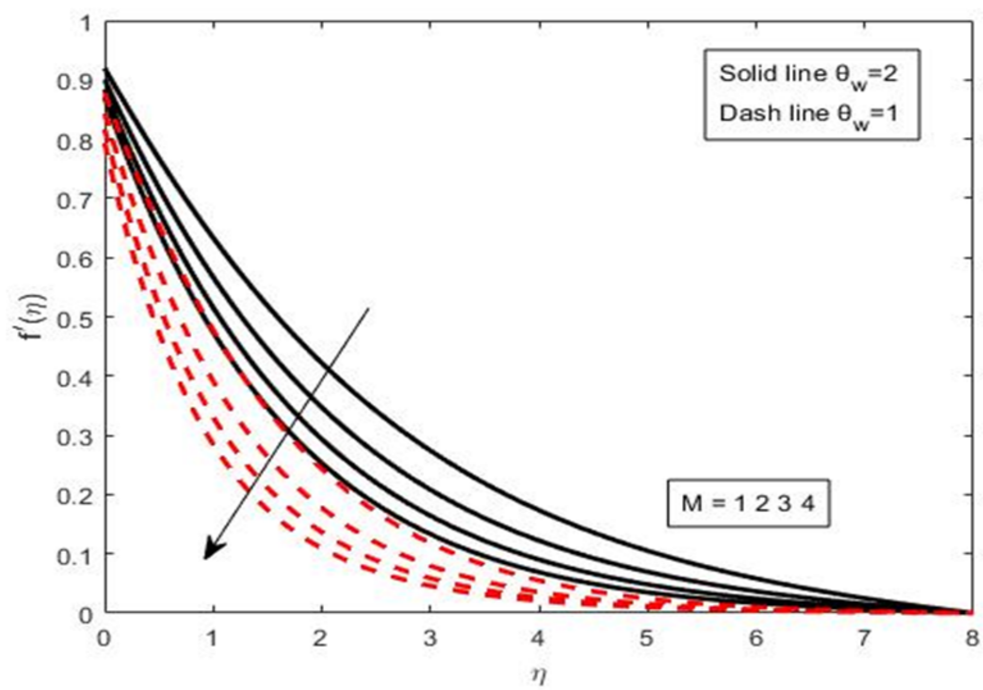

Fig 3. Results of M on Velocity

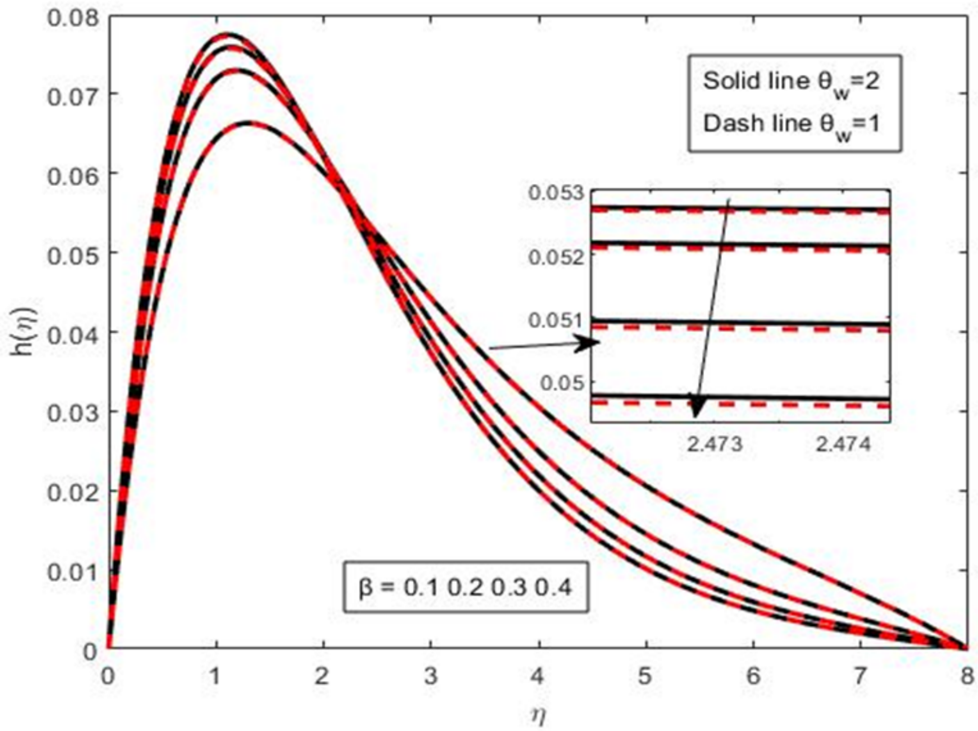

Fig 4. Results of β on angular velocity

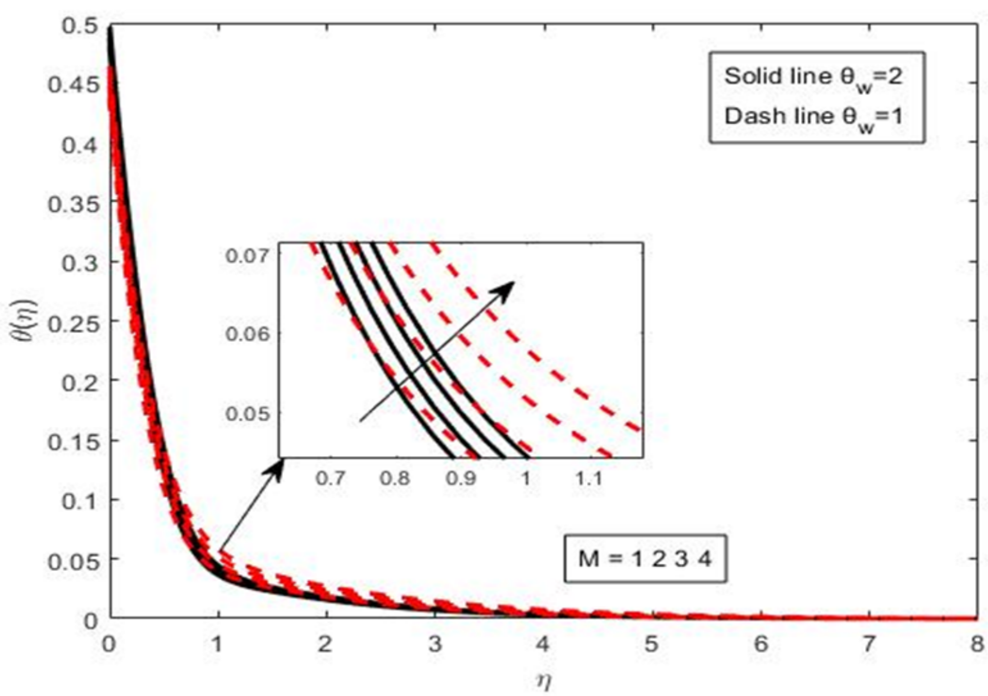

Fig 5. Results of M on calefaction

Table 1. Comparison values of Magnetic parameter in $-f''(0)$

M	Yousef[(22)]	Present Results
0.0	1.00139983	1.00014002
1.0	1.41422875	1.41423561
3.0	2.00000000	2.00001101
5.0	2.44948791	2.44950121

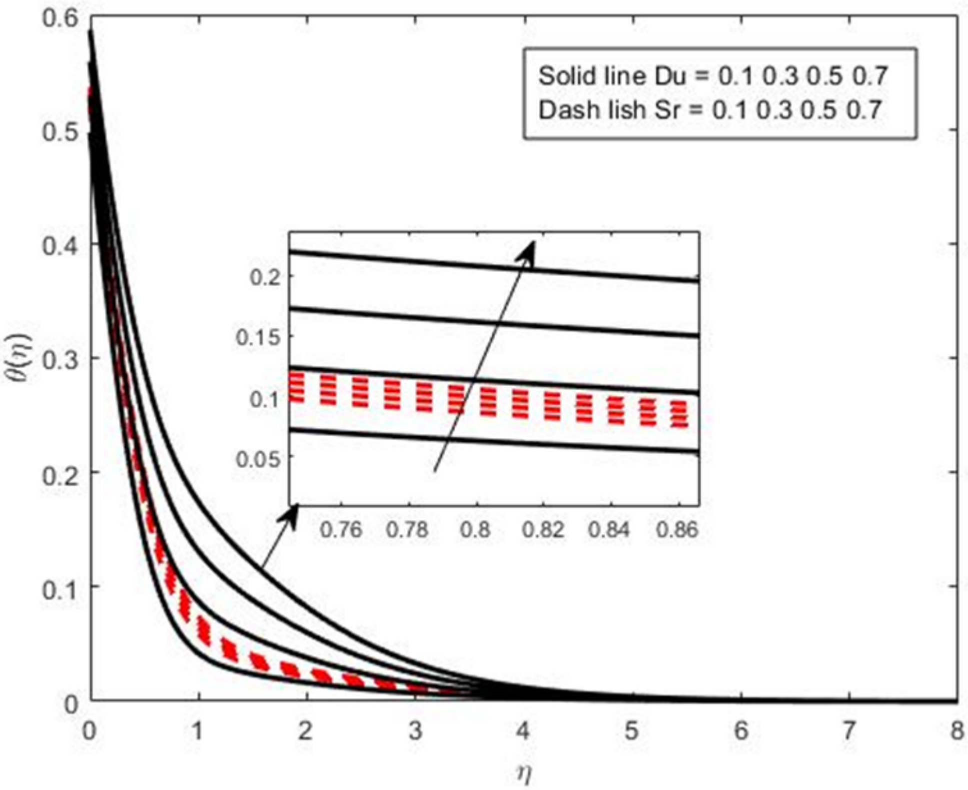

Fig 6. Results of $Du \wedge Sr$ on calefaction

is decreased on the extensive β, whilst $\theta(\eta), \phi(\eta)$ are increased for the upsurged β. Figure 3 ritual that the possessions of $M.f'(\eta)$ is decreased on the extensive. A force called drag force is often produced by M in the paradoxical migration of the flow. Figure 5 shows that M on temperature its increased for the upsurged M similar β.

Figures 6 and 7 illustrate the impact of the Dufour and Soret numbers, which quantify the ratio of energy flux due to mass concentration gradients. Physically, the Dufour effect represents the contribution of mass diffusion to thermal energy transfer. The results indicate that as the Dufour number increases, thermal energy transfer is enhanced, leading to a rise in fluid temperature. This occurs because mass flux influences heat flux, reinforcing the coupling between mass and energy transport. Simultaneously, the concentration decreases due to mass redistribution induced by this effect. This inverse relationship between temperature and concentration highlights the critical role of the Dufour number in governing heat and mass transfer interactions. Conversely, the Soret effect accounts for mass transport driven by a temperature gradient. The results reveal that both absorption and heating intensify with an increasing Soret number. This indicates that thermal gradients play a crucial role in enhancing fluid transfer processes, particularly in systems where heat and mass transfer mechanisms are interdependent. The physical basis of this behaviour lies in the differential movement of species within the fluid, where temperature gradients drive concentration variations, leading to improved mixing and transport efficiency. Additionally, the presence of a magnetic field introduces resistance to fluid motion due to the Lorentz force, which arises from the interaction between the electrically conducting fluid and the magnetic field. This force acts as a drag, reducing the overall flow velocity and increasing friction at the

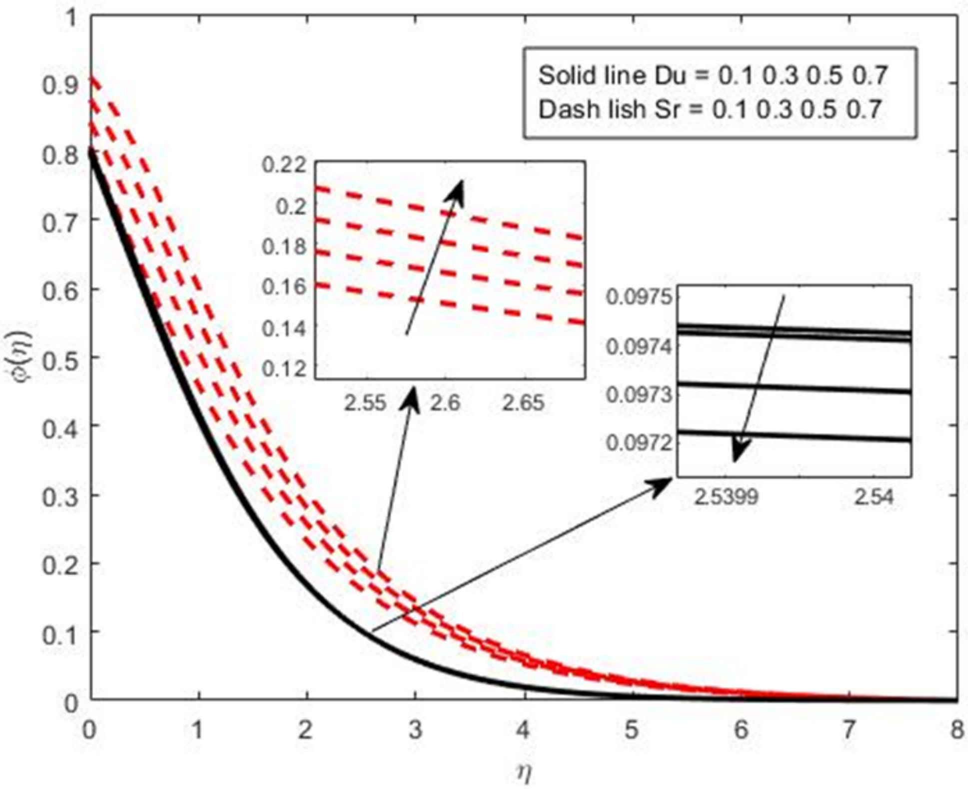

Fig 7. Results of $Du \wedge Sr$ on absorption

boundary. Such magnetic control is essential in engineering applications, particularly in scenarios where heat transfer and fluid dynamics must be regulated, such as in cooling systems, electromagnetic pumps, and industrial processes involving conductive fluids. Table 2 presents a detailed quantitative analysis of key dimensionless parameters, including the skin friction coefficient, Nusselt number, and Sherwood number. These parameters provide essential insights into the fluid's behaviour under different physical conditions. Variations in Skin frictionreflect changes in boundary layer characteristics due to factors like viscosity and magnetic influence, while fluctuations in the Nusselt and Sherwood numbers illustrate the efficiency of heat and mass transfer. Understanding these variations is crucial for optimizing thermal systems, improving heat exchanger performance, and refining fluid transport processes in practical applications.

The results of this study align with previous research[(7)],[(17)],[(21)], validating the accuracy of the proposed model. However, by integrating the effects of cross-diffusion (Dufour and Soret effects), micropolar fluid dynamics, and Casson rheology into a unified framework all of which were often treated separately in previous studies it results in significant advances. increase in the Sherwood and Nusselt values, demonstrating its ability to manage complex thermal system interactions. The addition of nonlinear stretching surfaces, which results in more realistic simulations, sets this work apart even further. All things considered, this work advances our understanding of heat and mass transmission in Casson nanofluids and offers a more comprehensive model for thermal system adaptation.

5 Conclusion

Casson nanofluids over nonlinearly stretched surfaces in an inclined magnetic field are numerically assessed, providing new information on developing heat transmission and mixing technologies. The major key findings are:

- The requirement for balance in advanced heat exchanger designs is highlighted by the fact that greater Soret numbers increase concentration levels while higher Dufour numbers cause concentration levels to fall.

Table 2. The values of C_{fx}, Nu and Sh on different physical parameters

M	β	Kr	Sc	Du	**Sr**	Nr	Grc	Bic	BiT	**C**$_{fx}$	**Nu**	**Sh**
1.0	0.1	0.1	0.5	0.1	0.1	0.1	0.5	0.5	0.5	-3.5317	2.6985	0.3946
2.0	0.1	0.1	0.5	0.1	0.1	0.1	0.5	0.5	0.5	-4.3827	2.6677	0.3836
3.0	0.1	0.1	0.5	0.1	0.1	0.1	0.5	0.5	0.5	-5.0844	2.6409	0.3745
4.0	0.1	0.1	0.5	0.1	0.1	0.1	0.5	0.5	0.5	-5.6863	2.6168	0.3668
0.1	**0.1**	0.1	0.5	0.1	0.1	0.1	0.5	0.5	0.5	-3.5247	2.6314	0.3973
0.1	**0.2**	0.1	0.5	0.1	0.1	0.1	0.5	0.5	0.5	-2.3573	2.6011	0.3852
0.1	**0.3**	0.1	0.5	0.1	0.1	0.1	0.5	0.5	0.5	-1.8833	2.5826	0.3783
0.1	**0.4**	0.1	0.5	0.1	0.1	0.1	0.5	0.5	0.5	-1.6190	2.5698	0.3737
0.1	0.1	**0.1**	0.5	0.1	0.1	0.1	0.5	0.5	0.5	-3.9466	2.6266	0.3575
0.1	0.1	**0.2**	0.5	0.1	0.1	0.1	0.5	0.5	0.5	-3.9733	2.6152	0.3915
0.1	0.1	**0.3**	0.5	0.1	0.1	0.1	0.5	0.5	0.5	-3.9963	2.6047	0.4218
0.1	0.1	**0.4**	0.5	0.1	0.1	0.1	0.5	0.5	0.5	-4.0163	2.5950	0.4493
0.1	0.1	0.1	**0.5**	0.1	0.1	0.1	0.5	0.5	0.5	-3.9385	2.6302	0.3659
0.1	0.1	0.1	**1.0**	0.1	0.1	0.1	0.5	0.5	0.5	-4.0584	2.5601	0.4673
0.1	0.1	0.1	**1.5**	0.1	0.1	0.1	0.5	0.5	0.5	-4.1114	2.4988	0.5315
0.1	0.1	0.1	**2.0**	0.1	0.1	0.1	0.5	0.5	0.5	-4.1412	2.4433	0.5794
0.1	0.1	0.1	0.5	**0.1**	0.1	0.1	0.5	0.5	0.5	-3.9733	2.6152	0.3915
0.1	0.1	0.1	0.5	**0.3**	0.1	0.1	0.5	0.5	0.5	-3.9348	2.4473	0.3977
0.1	0.1	0.1	0.5	**0.5**	0.1	0.1	0.5	0.5	0.5	-3.8977	2.2925	0.4035
0.1	0.1	0.1	0.5	**0.7**	0.1	0.1	0.5	0.5	0.5	-3.8619	2.1488	0.4088
0.1	0.1	0.1	0.5	0.1	**0.1**	0.1	0.5	0.5	0.5	-1.0995	2.4936	0.3840
0.1	0.1	0.1	0.5	0.1	**0.3**	0.1	0.5	0.5	0.5	-1.0752	2.4639	0.3149
0.1	0.1	0.1	0.5	0.1	**0.5**	0.1	0.5	0.5	0.5	-1.0519	2.4358	0.2483
0.1	0.1	0.1	0.5	0.1	**0.7**	0.1	0.5	0.5	0.5	-1.0293	2.4093	0.1838
0.1	0.1	0.1	0.5	0.1	0.1	**0.1**	0.5	0.5	0.5	-3.9862	1.9335	0.3841
0.1	0.1	0.1	0.5	0.1	0.1	**0.2**	0.5	0.5	0.5	-3.9733	2.6152	0.3915
0.1	0.1	0.1	0.5	0.1	0.1	**0.3**	0.5	0.5	0.5	-3.9603	3.2127	0.3980
0.1	0.1	0.1	0.5	0.1	0.1	**0.4**	0.5	0.5	0.5	-3.9472	3.7423	0.4036
0.1	0.1	0.1	0.5	0.1	0.1	0.1	**0.0**	0.5	0.5	-4.0018	2.6146	0.3922
0.1	0.1	0.1	0.5	0.1	0.1	0.1	**0.5**	0.5	0.5	-3.7013	2.6253	0.3954
0.1	0.1	0.1	0.5	0.1	0.1	0.1	**1.0**	0.5	0.5	-3.4083	2.6354	0.3985
0.1	0.1	0.1	0.5	0.1	0.1	0.1	**1.5**	0.5	0.5	-3.1220	2.6451	0.4014
0.1	0.1	0.1	0.5	0.1	0.1	0.1	0.5	**0.5**	0.5	-3.6788	2.6442	0.2320
0.1	0.1	0.1	0.5	0.1	0.1	0.1	0.5	**1.0**	0.5	-3.5955	2.6373	0.3209
0.1	0.1	0.1	0.5	0.1	0.1	0.1	0.5	**1.5**	0.5	-3.5517	2.6337	0.3681
0.1	0.1	0.1	0.5	0.1	0.1	0.1	0.5	**2.0**	0.5	-3.5247	2.6314	0.3973
0.1	0.1	0.1	0.5	0.1	0.1	0.1	0.5	0.5	**0.5**	-3.6153	1.0520	0.4398
0.1	0.1	0.1	0.5	0.1	0.1	0.1	0.5	0.5	**1.0**	-3.5778	1.7763	0.4198
0.1	0.1	0.1	0.5	0.1	0.1	0.1	0.5	0.5	**1.5**	-3.5482	2.2782	0.4064
0.1	0.1	0.1	0.5	0.1	0.1	0.1	0.5	0.5	**2.0**	-3.5247	2.6314	0.3973

- Complex control mechanisms are demonstrated when thermal-fluid dynamics combine with magnetic and Casson factors to decrease velocity while raising temperature and concentration.
- In comparison to earlier research, the suggested model, which combines Casson rheology, micropolar effects, and cross-diffusion dynamics, shows an increase in the Sherwood number and a rise in the Nusselt number.
- These contributions close important gaps in the study of non-Newtonian fluids and offer significant improvements in enhancing the efficiency of thermal systems for use in engineering and medicine.

Future work should explore experimental validation, turbulent flows, and additional factors such as thermal radiation to enhance practical applicability. This model can be expanded to include stagnation points and wavy surfaces for heat exchangers and aerodynamics, as well as cylindrical and spherical geometries for use in blood arteries, pipes, and porous channels. Its relevance to practical engineering and fluid mechanics research is increased by include effects like convective barriers, non-uniform heat sources, and variable transport qualities.Nomenclature(u, v)Velocity components (m/s)β_TThermal coefficient (K^{-1})β_cConcentration coefficient (m^3/mol)TFluid temperature (K)T_∞Uniform temperature (K), **C** Concentration fluid (kg/m^3)C_∞Uniform concentration (kg/m^3)αAngle of inclinationσElectric conductivity fluid (S/m)B_0Uniform magnetic field (T)gGravitational acceleration (m/s^2)K_1Permeability of the fluid (m^2)q'''Irregular heat parameter (W/m^3)D_mMass diffusivity (m^2/s)C_sConcentration susceptibility (m^3/mol)T_mMean temperature (K)B_{iT}Thermal Biot NumberB_{iC}Mass Biot NumberγVelocity slip parameter (m/s)G_{rT}Thermal Grashot numberG_{rc}Solutes Grashot number$M$Hartmann number$N_r$radiative parameterS_rSoret numberS_CSchmidt numberD_uDufour numberK_rChemical parameterq_rRadiative heat (W/m^2)KNon dimensional parameterP_rPrandtl number

6 Acknowledgement

The authors did not receive any support from any organization for the submitted work.

References

1) Shaheen N, Ramzan M, Alshehri A. Soret–Dufour impact on a three-dimensional Casson nanofluid flow with dust particles and variable characteristics in a permeable media. *Scientific Reports*. 2021;11:14513. doi:https://doi.org/10.1038/s41598-021-93797-2.
2) Amjad M, Zehra I, Nadeem S, Zehra I, Nadeem S, Abbas N. Thermal analysis of Casson micropolar nanofluid flow over a permeable curved stretching surface under the stagnation region. *Journal of Thermal Analysis and Calorimetry*. 2021;143:2485–2497. doi:https://doi.org/10.1007/s10973-020-10127-w.
3) Devi R, Sood S. Numerical analysis of the influence of an inclined magnetic field on the flow of Casson nanofluid across an exponentially stretching surface using the Darcy-Forchheimer model. *Indian Journal of Science and Technology*. 2023;16(44):4081–4089. doi:https://doi.org/10.17485/IJST/v16i44.2481.
4) Chun O, Raja MAZ, Naz S, Ahmad I, Akhtar R, Ali Y, et al. Dynamics of inclined magnetic field effects on micropolar Casson fluid with Lobatto IIIA numerical solver. *AIP Advances*. 2020;10(6):065023. doi:https://doi.org/10.1063/5.0004386.
5) Magesh V, Pushparaj S, Tamizharasi P. Numerical investigations of activation energy on the peristaltic transport of Carreau nanofluid through a curved asymmetric channel. *Physics of Fluids*. 2023;35(10):101906. doi:https://doi.org/10.1063/5.0167829.
6) Shevchuk IV. An analytical solution for convective heat transfer in conical gaps with either cone or disk rotating. *Physics of Fluids*. 2023;35(11):113117. doi:https://doi.org/10.1063/5.0179146.
7) Bafakeeh OT, Raghunath K, Ali F. Hall current and Soret effects on unsteady MHD rotating flow of second-grade fluid through porous media under the influences of thermal radiation and chemical reactions. *Catalysts*. 2022;12(10):1233. doi:https://doi.org/10.3390/catal12101233.
8) Chandrasekhar B, Lakshmi BS, Reddy MK. Casson-nano-magnetohydrodynamics boundary layer fluid flow towards a stretching sheet including the effects of cross diffusion, velocity, and thermal wall slips. *Journal of Nanofluids*. 2022;11:915–923. doi:https://doi.org/10.1166/jon.2022.1883.
9) Kesavaiah DC, Nagaraju V, Venkateswarlu B. Investigating the influence of chemical reaction on MHD-Casson nanofluid flow via a porous stretching sheet with suction/injection. *Science, Engineering and Technology*. 2023;3(2):47–62. doi:https://doi.org/10.54327/set2023/v3.i2.76.
10) Deepthi VVL, Lashin MMA, Kumar NR. Recent development of heat and mass transport in the presence of Hall, ion slip, and thermos diffusion in radiative second-grade material: Application of micromachines. *Micromachines*. 2022;13(10):1566. doi:https://doi.org/10.3390/mi13101566.
11) Ganjikunta A, Kommaddi H, Bhajanthri V, Raghunath K. An unsteady MHD flow of a second-grade fluid passing through a porous medium in the presence of radiation absorption exhibits Hall and ion slip effects. *Heat Transfer*. 2023. doi:https://doi.org/10.1002/htj.22716.
12) Gopal D, Saleem S, Jagadha S. Numerical analysis of higher-order chemical reaction on electrically MHD nanofluid under the influence of viscous dissipation. *Alexandria Engineering Journal*. 2021;60:1861–1871. doi:https://doi.org/10.1016/j.aej.2020.11.034.
13) Rasool G, Chamkha AJ, M T. Darcy-Forchheimer relation in Casson type MHD nanofluid flow over non-linear stretching surface. *Propulsion and Power Research*. 2021. doi:https://doi.org/10.1016/j.jppr.2020.04.003.
14) Jawad M, Mebarek-Oudina F, Vaidya H, Prashar P. Influence of bioconvection and thermal radiation on MHD Williamson nano Casson fluid flow with the swimming of gyrotactic microorganisms due to porous stretching sheet. *Journal of Nanofluids*. 2022;11:500–509. doi:https://doi.org/10.1166/jon.2022.1863.
15) Kodi R, Ganteda C, Dasore A. Influence of MHD mixed convection flow for Maxwell nanofluid through a vertical cone with porous material in the existence of variable heat conductivity and diffusion. *Case Studies in Thermal Engineering*. 2023;44:102875. doi:https://doi.org/10.1016/j.csite.2023.102875.
16) Kumar B, Srinivas S. Unsteady hydromagnetic flow of Eyring–Powell nanofluid over an inclined permeable stretching sheet with joule heating and thermal radiation. *Journal of Applied and Computational Mechanics*. 2020;6:259–270. doi:https://doi.org/10.22055/jacm.2019.29520.1608.
17) Reddy VV, Ganta S, Raghunath K. Effects of Hall current, activation energy, and diffusion thermos of MHD Darcy-Forchheimer Casson nanofluid flow in the presence of Brownian motion and thermophoresis. *Journal of Advanced Research in Fluid Mechanics and Thermal Sciences*. 2023;105(2):129–145. doi:https://doi.org/10.37934/arfmts.105.2.129145.

18) Rafique K, Imran MA, Anwar MI. Energy and mass transport of Casson nanofluid flow over a slanted permeable inclined surface. *Journal of Thermal Analysis and Calorimetry*. 2021. doi:https://doi.org/10.1007/s10973-020-10481-9.
19) Sutkar P. Flow characteristics of Casson nanofluid over a moving wedge. *Indian Journal of Science and Technology*. 2024;17(13):1349–1356. doi:https://doi.org/10.17485/IJST/v17i13.234.
20) Ramya N, Deivanayaki M. Numerical simulation of Casson micropolar fluid flow over an inclined surface through a porous medium. *Journal of Mines, Metals & Fuels*. 2023;71(11):2143–2149. Available from: https://informaticsjournals.com/index.php/jmmf/article/view/36269.
21) Ramya N, Deivanayaki M. Heat radiation on Casson nanofluid flow over an inclined stretching surface with heat and mass diffusions;vol. 414. 2024. doi:https://doi.org/10.1007/978-3-031-69970-2_27.
22) Yousef NS, Megahed AM, Ghoneim NI. Chemical reaction impact on MHD dissipative Casson-Williamson nanofluid flow over a slippery stretching sheet through porous medium. *Alexandria Engineering Journal*. 2022;61:10161–10170. doi:https://doi.org/10.1016/j.aej.2022.03.032.
23) Manohar GR, Venkatesh P, Gireesha BJ, Ramesh GK. Numerical treatment for Casson liquid flow in a microchannel due to porous medium: A hybrid nanoparticle aspect. *Proceedings of the Institution of Mechanical Engineers, Part C: Journal of Mechanical Engineering Science*. 2022;236(2):1293–1303. doi:https://doi.org/10.1177/09544062211008933.
24) Ramesh GK, Roopa GS, Rauf A, Shehzad SA, Abbasi FM. Time-dependent squeezing flow of Casson-micropolar nanofluid with injection/suction and slip effects. *International Communications in Heat and Mass Transfer*. 2021;126:105470. doi:https://doi.org/10.1016/j.icheatmasstransfer.2021.105470.